American Journal of Aerospace Engineering
2018; 5(2): 96-105
http://www.sciencepublishinggroup.com/j/ajae
doi: 10.11648/j.ajae.20180502.14
ISSN: 2376-4813 (Print); ISSN: 2376-4821 (Online)

Adapting SE (3) Nonlinear Geometric Method to Control Single-Tri Rotors with Integrator

Dinh-Thinh Hoang[1], Thi-Hong-Hieu Le[1], Ngoc-Hien Nguyen[2]

[1]Department of Aerospace Engineering, Ho Chi Minh City University of Technology – VNU-HCM, Ho Chi Minh City, Vietnam
[2]Department of Mathematical Sciences, School of Sciences, RMIT University, Melbourne, Australia

Email address:
hdinhthinh@gmail.com (Dinh-Thinh H.), honghieu.le@hcmut.edu.vn (Thi-Hong-Hieu L.), hien.nguyen@rmit.edu.au (Ngọc-Hien N.)

To cite this article:
Dinh-Thinh Hoang, Thi-Hong-Hieu Le, Ngoc-Hien Nguyen. Adapting SE (3) Nonlinear Geometric Method to Control Single-Tri Rotors with Integrator. *American Journal of Aerospace Engineering*. Vol. 5, No. 2, 2018, pp. 96-105. doi: 10.11648/j.ajae.20180502.14

Received: October 14, 2018; **Accepted**: October 18, 2018; **Published**: November 21, 2018

Abstract: This paper presents a new method for controlling tri rotor-type unmanned aerial vehicles (UAV) adapted from the SE (3) nonlinear geometric method for quadrotor-type UAV. Like its predecessor, the control strategy for single tri rotors is realized in a hierarchical architecture, containing both attitude controller and position controller. As a basis, the mathematical dynamics of the tri rotor is given in form of rotation matrix that ensures the algorithm is independent from any specific representation, such as Euler angle or quaternion. Assumption about primary thrust component is made to decouple the equations of the controllers to find an appropriate reference target for the attitude controller. An integral action is proposed to alleviate the steady-state error that arises from incorrect modelling due to simplification. This is justified by a Lyapunov function that also yields additional conditions for parameter gains setup. Output of the controller includes desired torque components, as well as total thrust magnitude. It is from this point that divergence from the original method for quadrotors becomes prominent. A numerical solver is introduced to yield the desired motors' angular speed and tail servo angle. Some numerical examples implemented on MATLAB/Simulink illustrate that the controller is able to correct steady-state error and gives quick response, just like its quadrotor-type counterpart.

Keywords: Tri Rotor, Geometric, Nonlinear, Control, SE (3), SO (3).

1. Introduction

Unmanned aerial vehicles (UAVs) are becoming more and more popular because of their benefits. For instance, UAVs have increased their existence through various activities such as photography, 3D mapping [1], remote sensing [2], management and inspection of giant assets such as a power line or a complex construction. Moreover, UAVs are believed to be helpful in disaster responses, providing preliminary supplies for those in emergency situations before further help arrives [3]. Developments of compact sensors, batteries, and microprocessors have been the main forces behind the growing momentum of UAVs in recent years that crystallized in the invention of many UAV designs. Among those, rotary wing UAVs account for a significant portion of interest by virtue of hovering and Vertical Take-off and Landing (VTOL) capabilities, which enables the UAV to be used in complicated navigation environment, such as inside a building or in the mountains.

Tri-rotor is a rotary-wing type UAV which has three propellers to generate the lift, as well as to control the attitude and position. This design is further divided into various classes such as single tri-rotor [4] and coaxial tri-rotor. The single tri-rotor has a servo motor on one of the arms that connect the rotors with the hub to tilt the rotor to some angles, providing the yaw stability (Figure 1). Furthermore, this design allows the tri-rotor to perform the tight-turn and to keep the UAV more stable.

An apparent issue of single tri rotor design is its nonlinear dynamics. The interest in tri-rotor design has just picked up recently, thus comparing to quadrotors, literature about tri-rotor control is not as rich. However, several control algorithms, both linear and nonlinear, are available. A control strategy in [6] proposed a scheme for the mixing signals and design PID controllers. Optimal LQR control for the regulation of individual roll, pitch, and yaw channel is attempted in [7]. A fuzzy logic controller can also be used in

a hybrid scheme to augment the tri-rotor's dynamic response [8, 9]. The study in [7] also proposed a strategy for back-stepping control of the attitude angles while a full position tracking control can be found in [10]. A research in [11] presented a feedback linearization, in junction with a H^{∞} loop shaping controller for controlling the tri-rotor.

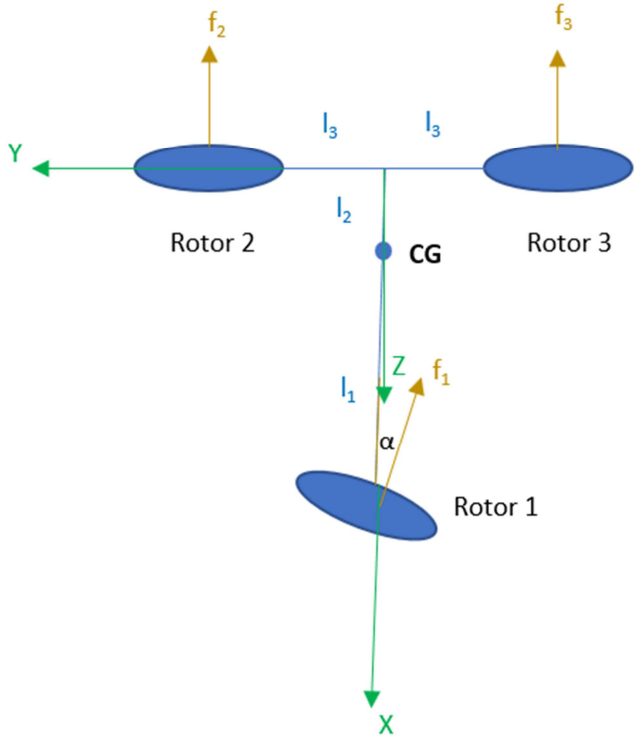

Figure 1. *Single tri rotor model.*

Geometric control method on SE (3) [12] exploits the Lie group structure of the Special Orthogonal Group SO (3) to create an algorithm that exhibits almost global stability for quadrotor UAVs. The algorithm is further developed to be adaptable to the changes in mass and moment of inertia and proven to be robust and fast, capable of performing aggressive maneuverings [13]. Foundation of the method is coordinate-free i.e. does not depend on a particular representation of attitude such as 0 Euler angles or quaternions. The controller comprises of two separate controllers: attitude controller and position controller, realized through the Lyapunov direct method. Since the rotor plane of a quadrotor does not change, this design has provided an intrinsic mechanism to connect two separate controllers in an easy way. For single tri-rotor, the nonlinearity in the dynamics model implies that the coupling between the thrust vector and aircraft attitude cannot be broken, unless an assumption about the large thrust magnitude in the vertical orientation is made. Inaccurate modelling resulted in the appearance of steady-state error, which can be circumvented by introducing an integral action.

This paper presents a new method to adapt the SE (3) nonlinear geometric controller for quadrotors to tri rotors. The new algorithm promises all the same advantages as the original algorithm, which are fast responsiveness and robustness to disturbances, but at the cost of heightened computational cost – due to the implementation of a numerical solver.

The rest of this paper is organized as follows. In Section 2, a dynamic model for single tri-rotor is presented. In Section 3, a quick recall of some important results from [12, [14] and a description for a new position controller with an integrator to improve robustness are carried out. In Section 4, results of the numerical simulation using MATLAB/Simulink are presented along with discussions. Finally, some concluding remarks are provided in Section 5.

2. Dynamics Modelling

The dynamics model of the tri rotor is based on a set of differential equations that governs a typical 6 degree-of-freedom in three-dimensional space. Let

$$\xi = (x, y, z)^T$$

be the position of aircraft's centre of gravity (CG) with respect to a Cartesian inertial frame, and

$$v = \dot{\xi} \tag{1}$$

be the velocity of the aircraft in the same frame. Newton's second law gives:

$$m\dot{v} = F_e \tag{2}$$

where F_e denotes the net force vector acting on the aircraft written with respect to the inertial frame.

Figure 2. *Aircraft's position and attitude are represented by the centre of gravity's position in the inertial frame and a rotation transformation R that transforms the body frame to inertial frame.*

The aircraft's attitude can be depicted by the rotation transformation $R \in SO(3) \subset GL(3)$ that takes an arbitrary vector from the body frame and converts it into a vector in the inertial frame. Its dynamics is given by:

$$\dot{R} = R(sk(\Omega)) \tag{3}$$

where Ω is the angular rates in the body frame and $sk(\,)$ denotes the skew-symmetric transformation mapping, defined as:

$$sk\left(\begin{bmatrix} a \\ b \\ c \end{bmatrix}\right) = \begin{bmatrix} 0 & -c & b \\ c & 0 & -a \\ -b & a & 0 \end{bmatrix} \tag{4}$$

Finally, the rotational dynamics of the aircraft can be

expressed as:

$$J\dot{\Omega} = -\Omega \times J\Omega + \tau \tag{5}$$

where J is the moment of inertial matrix of the aircraft, τ is the torque applying on the aircraft around its centre of gravity.

Thus, equations (1), (2), (3) and (5) form a complete set of tri rotor's dynamics:

$$\begin{aligned} \dot{\xi} &= v \\ m\dot{v} &= F_e \\ \dot{R} &= Rsk(\Omega) \\ J\dot{\Omega} &= -\Omega \times J\Omega + \tau \end{aligned} \tag{6}$$

The force F_e is given as:

$$F_e = mge_3 + RF_{ab} \tag{7}$$

where $e_3 = [0\ 0\ 1]^T$ and according to [6]:

$$F_{ab} = \begin{bmatrix} 0 \\ f_1 \sin\alpha \\ -f_2 - f_3 - f_1 \cos\alpha \end{bmatrix} \tag{8}$$

is the thrust vector written with respect to the body frame and:

$$\tau = \begin{bmatrix} -l_3(f_2 - f_3) \\ -l_2(f_2 + f_3) + l_1 f_1 \sin\alpha \\ l_1 f_1 \sin\alpha - \tau_1 \cos\alpha + \tau_2 - \tau_3 \end{bmatrix} \tag{9}$$

is the torque around the aircraft's CG with respect to body frame [6]. The length l_1, l_2, l_3 are described in Figure 1.

By using simplified model, the thrust created by each rotor is proportional to its angular speed and so is the torque:

$$f_i = c_T \omega_i^2, i \in [1,2,3]$$

$$\tau_i = c_Q \omega_i^2, i \in [1,2,3]$$

The whole system has 4 inputs to control: individual rotor angular speed f_1, f_2, f_3 and servo tail angle α. The response of each variable must be quick enough, otherwise the aircraft would fail to track the reference signal.

3. The SE (3) Nonlinear Controller

Adapting from the hierarchy described in [12], the controller is made up of attitude controller and position controller respectively. Additionally, there is a Command Signal Resolver (CSR) block, which is a numerical solver to solve for desired rotor speed and servo tail angle. Figure 3 depicts the holistic view of the entire control system.

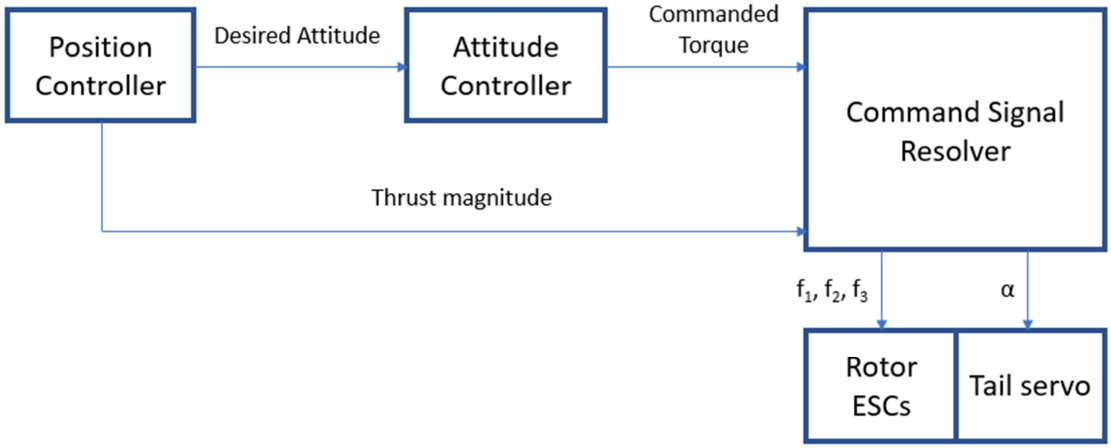

Figure 3. *Hierarchy of the control system.*

3.1. Attitude Tracking Controller

The attitude controller takes the desired attitude, expressed as the rotation matrix R_d, along with desired angular rates Ω_d expressed in body frame as reference signal. Feedback signal includes the moment of inertia matrix J, current angular rates obtained from the gyroscopes. From [12] and [14], the control law is as follows:

$$\begin{aligned} \tau = {} & sk(\Omega)J\Omega + J(-k_r e_R - k_\Omega e_\Omega \\ & -sk(\Omega)R^T R_d \Omega_d + R^T R_d \dot{\Omega}_d) \end{aligned} \tag{10}$$

where e_R is the error between current and desired aircraft attitude:

$$e_R = \frac{1}{2} sk^{-1}\left(R_d^T R - R^T R_d\right) \tag{11}$$

and e_Ω describes the instant time evolution of attitude error:

$$e_\Omega = \Omega - R^T R_d \Omega_d \tag{12}$$

Also, from [14], the initial condition for tracking is:

$$\frac{1}{2} \| e_\Omega(0) \|^2 \leq 2k_r - k_r \Psi(0)$$

where

$$\Psi = \frac{1}{2} trace(I - R_d^T R)$$

and the sufficient condition for the gain k_r, k_Ω to satisfy is:

$$\begin{bmatrix} k_\Omega - 1 & -\frac{1}{2} \\ -\frac{1}{2} & k_r \end{bmatrix}$$

is positive definite.

It can be proven that if $\Psi < 2$ corresponds to attitude error angle less than 180^o, the origin is exponentially stable [12, 14]. This property can be leveraged to perform aggressive manoeuvres from some pre-programmed motions.

3.2. Position Tracking Controller

Differences between single tri rotors and quadrotors make the problem subtler from here. To be able to track some trajectories, the position controller has to generate a desired attitude so that the attitude controller can track. In fact, it is only the thrust vector (the normalised vector pointing in the direction of total force generated by all rotors) that is of concern for position tracking. Construction of the entire desired attitude requires an additional vector, which can be deduced from the input yaw angle.

Due to the under-actuated nature of the system, we cannot freely decouple the attitude tracking and position tracking. This problem is further complicated by the coupling between thrust direction and aircraft attitude through inputs f_1, f_2, f_3 and α. In other words, we cannot obtain an immediate desired attitude just by having a thrust vector and a yaw angle as in the quadrotor's case. Any attempt would require an iterative process that solves all the inputs and the aircraft desired attitude at the same time. This would bring heightened computational cost to the processor on board, as well as additional difficulties in analysis. However, since most of the thrust is given out in the direction perpendicular to the rotor plane, we can neglect the other components and use the same approach as for a quadrotor.

$$F_{ab} = \begin{bmatrix} 0 \\ f_1 \sin\alpha \\ -f_2 - f_3 - f_1 \cos\alpha \end{bmatrix} \approx \begin{bmatrix} 0 \\ 0 \\ -f_2 - f_3 - f_1 \cos\alpha \end{bmatrix} \quad (13)$$

This is one source of inaccuracy in modelling. External disturbances may cause additional inaccuracy, resulting in enlarged steady-state error. To improve robustness, we turn to the implementation of an integrator. Let

$$e_x = x - x_d \quad (14)$$

as the translational position error between the current and desired position. It can be proven that the following thrust vector is required for asymptotic position tracking:

$$TV = \frac{mge_3 + mk_x e_x + mk_v e_v + mk_i \chi - m\dot{v}_d}{\| mge_3 + mk_x e_x + mk_v e_v + mk_i \chi - m\dot{v}_d \|} \quad (15)$$

and thrust magnitude is:

$$f = (mge_3 + mk_x e_x + mk_v e_v + mk_i \chi - m\dot{v}_d) \cdot \mathrm{Re}_3 \quad (16)$$

where χ is integration of e_x:

$$\chi = \int e_x dt$$

The necessary conditions for asymptotic tracking are:

$$\| \dot{v}_d - ge_3 \| < B_{max} \quad (17)$$

$$\| \chi \| < \| \chi \|_{max} \quad (18)$$

$$\| e_x \| < \| e_x \|_{max} \quad (19)$$

$$\frac{1}{2} \| e_\Omega(0) \| < \eta k_r - k_r \Psi(0) \quad (20)$$

where $\eta = 1 - \cos\alpha$ with α the maximum eigen-angle, limited to less than $\pi/2$. The controller parameters $k_r, k_x, k_v, k_\Omega, k_i$ must also satisfy the following identity:

$$\min(eig(W_2)) > \frac{4 \| W_T \|_2^2}{\min(eig(W_1))} \quad (21)$$

where

$$W_1 = \begin{bmatrix} k_\Omega - 1 & -\frac{1}{2} \\ -\frac{1}{2} & k_r \end{bmatrix} \quad (22)$$

$$W_2 = \begin{bmatrix} mk_i - c_1 k_x & \frac{1}{2}(c_2 + mk_x) \\ \frac{1}{2}(c_2 + mk_x) & mk_v - c_1 \end{bmatrix} \quad (23)$$

and

$$W_T = \frac{1}{1 - \alpha_0} \begin{bmatrix} 0 & c_1 k_i \| \chi \|_{max} + c_1 B_{max} \\ 0 & mB_{max} + c_1 k_v + mk_i \| \chi \|_{max} \end{bmatrix} \quad (24)$$

It is required that matrices W_1, W_2, W_T are positive definite. Additional conditions also require the following matrix positive definite:

$$M_1 = \begin{bmatrix} \frac{1}{2} c_1 k_i & \frac{1}{2} mk_i \\ \frac{1}{2} mk_i & c_2 \end{bmatrix} \quad (25)$$

and

$$M_2 = \begin{bmatrix} mk_x + c_1 k_v + c_2 & \frac{1}{2} c_1 \\ \frac{1}{2} c_1 & \frac{1}{2} m \end{bmatrix} \quad (26)$$

The existence of any (c_1, c_2) that satisfies the above conditions will guarantee the asymptotic stability of the origin with respect to the conditions given in (17-20). The Lyapunov candidate function for the position controller to yield the above results is:

$$V_4 = \frac{m}{2(1-\alpha_0)} \| e_v \|^2 + \frac{1}{2(1-\alpha_0)} (mk_x + c_1 k_v + c_2) \| e_x \|^2 + c_1 e_x \cdot e_v + \frac{1}{2} c_1 k_i \chi^2 + m k_i \chi \cdot e_x$$

The last two terms (and term $c_2\|e_x\|^2$) of the Lyapunov function V_4 is to accommodate the integrator. Formal proof of this statement is given in [15] while some of the conditions for signal boundedness can be found in [14].

The introduction of an integrator complicates the analysis process; an extra care has to be considered so that the maximum output of the integrator is well regulated with respect to condition (17). This can be achieved via introduction of a saturator at the output of the integrator. Moreover, to prevent excess overshooting due to integrator wind-up, we adopt a very simple mechanism that stops the accumulation process whenever there is at least one rotor is saturated at maximum output.

To generate the desired attitude, we have to take into account the input yaw angle to generate one additional vector, denoted as PDV, which is constructed by multiplying the rotation matrix expressed by Euler angles as $\phi = 0, \theta = 0, \psi = \psi(t)$ with $[1, 0, 0]^T$. This vector is projected onto the plane perpendicular to thrust vector to yield a concrete vector called DDV as follows:

$$DDV = -sk(T)(sk(T)PDV) \tag{27}$$

The remaining vector of the orthonormal axis system is taken as the cross product of the thrust vector and DDV:

$$V = sk(T)DDV \tag{28}$$

Finally, the desired attitude is:

$$R_d = [T, DDV, V] \tag{29}$$

i.e. the vectors are stacked horizontally.

3.3. Numerical Solver

For the quadrotor's case, the input command signal for the angular speed of the rotors can be found directly by solving a system of linear equations which can be very efficiently achieved. For the single tri-rotors, we need to have an additional solver to obtain these data numerically (Figure 4).

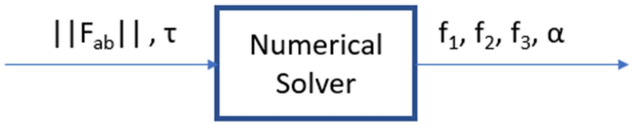

Figure 4. *Inputs and outputs of the numerical solver.*

The Newton-Raphson method is adopted to solve the nonlinear system of equations:

$$\begin{aligned} \tau_1 &= -l_3(f_2 - f_3) \\ \tau_2 &= -l_2(f_2 + f_3) + l_1 f_1 cos\alpha \\ \tau_3 &= l_1 f_1 sin\alpha - \tau_1 cos\alpha + \tau_2 - \tau_3 \\ \| F_{ab} \|^2 &= (f_1 sin\alpha)^2 + (f_2 + f_3 + f_1 cos\alpha)^2 \end{aligned} \tag{30}$$

If we use f_i as an input, the relationships are:

$$f_i = c_T \omega_i^2, i \in [1,2,3]; \quad \tau_i = c_Q \omega_i^2, i \in [1,2,3]$$

It is possible to rewrite the third equation of (30) as:

$$\tau_3 = l_1 f_1 \sin\alpha - \frac{c_T}{c_Q}(f_1 cos\alpha + f_2 - f_3) \tag{31}$$

The Newton-Raphson method involves finding the Jacobian of the system as follows:

$$\begin{bmatrix} \frac{\partial g_i}{\partial f_1} & \frac{\partial g_i}{\partial f_2} & \frac{\partial g_i}{\partial f_3} & \frac{\partial g_i}{\partial f_\alpha} \end{bmatrix} \tag{32}$$

in particular:

$$J = \begin{bmatrix} 0 & -l_3 & l_3 & 0 \\ l_1 cos\alpha & -l_2 & -l_2 & -l_1 f_1 \sin\alpha \\ l_1 \sin\alpha - \frac{c_T}{c_Q}\cos\alpha & -\frac{c_T}{c_Q} & \frac{c_T}{c_Q} & f_1\left(l_1 \cos\alpha + \frac{c_T}{c_Q}\sin\alpha\right) \\ 2(f_1 + \cos\alpha(f_2 + f_3)) & 2(f_2 + f_3 + f_1 cos\alpha) & 2(f_2 + f_3 + f_1 cos\alpha) & -2(f_2 + f_3) f_1 sin\alpha \end{bmatrix} \tag{33}$$

Starting from some initial value:

$$\begin{bmatrix} f_1 \\ f_2 \\ f_3 \\ \alpha \end{bmatrix}_0$$

we apply the following iterative formula:

$$\begin{bmatrix} f_1 \\ f_2 \\ f_3 \\ \alpha \end{bmatrix}_{n+1} = \begin{bmatrix} f_1 \\ f_2 \\ f_3 \\ \alpha \end{bmatrix}_n - J^{-1}F \tag{34}$$

where

$$F = \begin{bmatrix} -l_3(f_2 - f_3) \\ -l_2(f_2 + f_3) + l_1 f_1 cos\alpha \\ l_1 f_1 sin\alpha - \tau_1 cos\alpha + \tau_2 - \tau_3 \\ (f_1 sin\alpha)^2 + (f_2 + f_3 + f_1 cos\alpha)^2 \end{bmatrix} \quad (35)$$

The Newton-Raphson method has a fundamental weak point: it is not guaranteed to converge if the initial solution is not close enough to the solution. However, during simulations we found that an initial condition set at trimmed flight condition always yield a desirable performance with convergence achieved in less than 3 iterations.

4. Numerical Simulations

To demonstrate the effectiveness of the proposed approach, two simulations are conducted. The first simulation is the hovering test to examine the integrator in action. The second one is the trajectory tracking, whose sample trajectory is given in [14].

MATLAB/Simulink is employed to test the numerical examples. The parameters of a single tri-rotor UAV are given in Table 1.

The controller gains are setup as in Table 2.

For each of the following scenarios, we will compare the numerical results with and without the integration action (equivalent to setting k_i to 0 or 1.2).

4.1. Hovering Flight

In the hovering test, the UAV is placed at the origin, with zero initial translational and angular velocities and acceleration. In the first case, we simulate the drone response with respect to zero integration (which corresponds to $k_i = 0$). The result is given in Figure 5.

Table 1. *Single Tri rotor physical parameters.*

Parameter	Symbol	Value	Unit
Mass	m	1.12	kg
Gravitational acceleration	g	9.81	m/s^2
Thrust coefficient	c_T	1.4865e-7	kg.m
Torque coefficient	c_Q	2.9250e-9	$kg.m^2$
Moment of inertia	J	$\begin{bmatrix} 0.0095 & 0 & 0 \\ 0 & 0.0095 & 0 \\ 0 & 0 & 0.0186 \end{bmatrix}$	$kg.m^2$
Arm's length l_1	l_1	0.35	m
Arm's length l_2	l_2	0.35	m
Arm's length l_3	l_3	0.35	m

Table 2. *Single Tri rotor controller parameters.*

Parameter	Symbol	Value
Sampling time	T_s	1/60s
Frequency of controller's main loop	f_s	60Hz
Frequency of numerical solver	f_n	720Hz, equivalent to 12 iterations per input
Position proportional gain	k_x	5.6
Position derivative gain	k_v	2.8
Position integration gain	k_i	0 or 1.2, depends on the case
Attitude proportional gain	k_r	12.8
Attitude rate gain	k_Ω	7.2

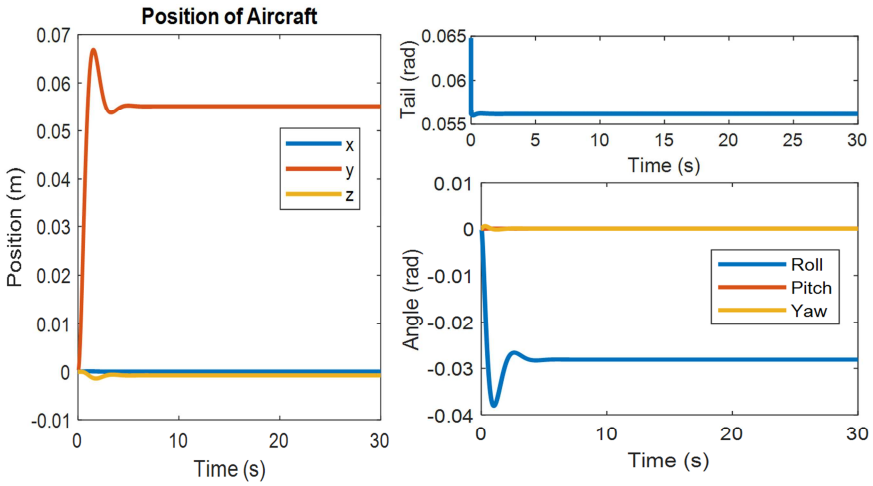

(a) Position (b) Tail angle and Euler angles

Figure 5. *Response of the aircraft in hover condition with no integration.*

Figure 5 showed that the equilibrium state of the drone does not coincide with zero roll, pitch and yaw angles. To prevent the tri-rotor from yawing due to the lack of counter rotating torque, the tail must be deflected to a small angle of 0.056 rad. However, this action leads to the existence of a horizontal force which tends to drift and roll the drone away. Therefore, the drone has to change its attitude to maintain the equilibrium between all forces and torques.

Although the simulation has yet to introduce any external disturbance, the steady state errors still appear across y and z components of the drone's position. This contributes to the inaccurate modelling due to the assumption that the thrust vector stays in the z axis, perpendicular to the rotor's plane in the body frame. Additional disturbance may enlarge this steady state errors, thus an integration is desired to increase the robustness of the control algorithm.

Setting k_i = 1.2 activates the integrator. The integrator accumulates the steady state error and provides a mechanism to reduce the error with time (Figure 6).

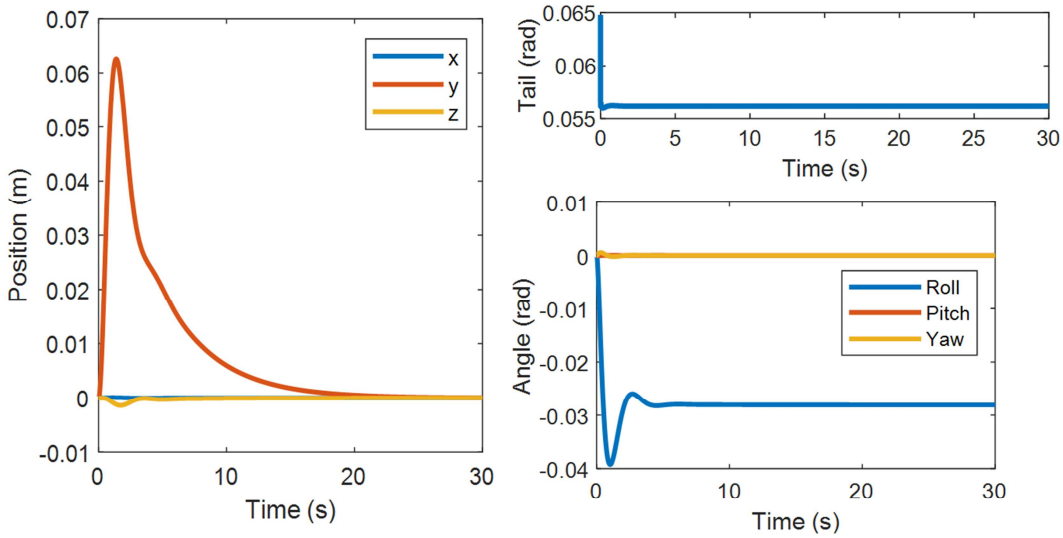

(a) Position (b) Tail angle and Euler angles

Figure 6. *Response of the aircraft in hover condition with integration.*

The integrator now drives the steady state error exponentially to zero. Although the response of the attitude angles seems similar to no integration case, there is a slowly decaying trend that is not quite visible in the graphs as shown in Figure 6.

4.2. Trajectory Tracking Flight

The sample trajectory to track is adopted from [14]. The trajectory is linearly interpolated from a table of desired position of the drone by time (Figure 7). Every single segment in the trajectory is travelled in 5 seconds.

Since the data is linearly interpolated, the reference signal has infinite acceleration command at 5n seconds, with $n \in (0,1,2,3,4,5,6)$. This acceleration is saturated across the implemented model. With no integration i.e. setting k_i to zero, the controller's response is obtained and plotted in Figure 8.

Figure 8 showed that the steady state error can be found in the y and z component, just like the hovering case. Similar the quadrotor's case, the response of the tri-rotor is quick with minimal delay or transient time, which is a strong point of this controller family.

Figure 9 reveals a subtle insight. The $||e_R||$ term corresponds to the performance of the attitude controller. The attitude controller is capable of driving the attitude error to zero, in contrast with position controller. This reiterates the point that the steady-state error stem from the trajectory tracking process is solely due to the approximation of thrust vector direction in the position controller and does not affect the attitude controller. A future work can be developed using the fact that the introduction of an integrator in the attitude tracking may also increase the robustness against disturbances, especially the torque disturbances.

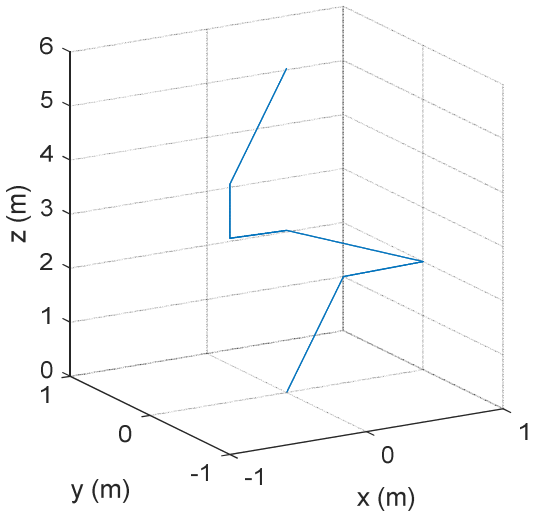

Figure 7. *Sample trajectory to track.*

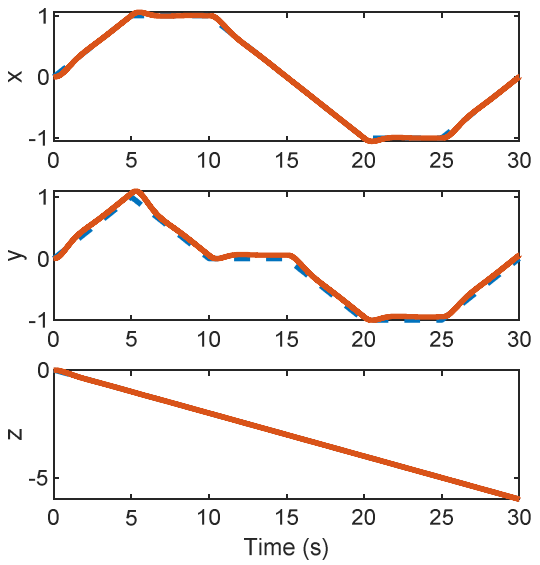

(a) Time response

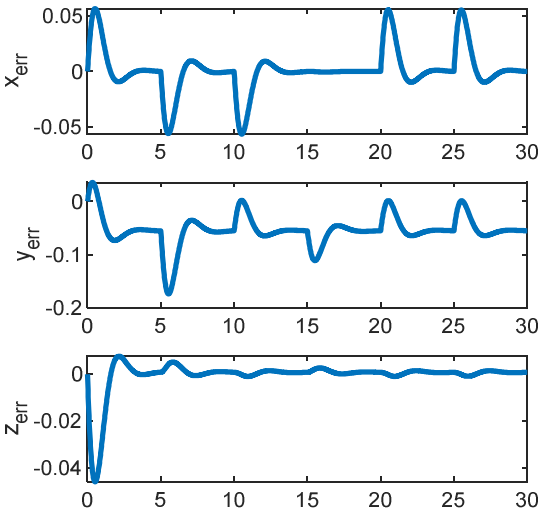

(b) Error response

Figure 8. *Aircraft's position response (no integrator) with time. Dashed lines indicate reference trajectory to track.*

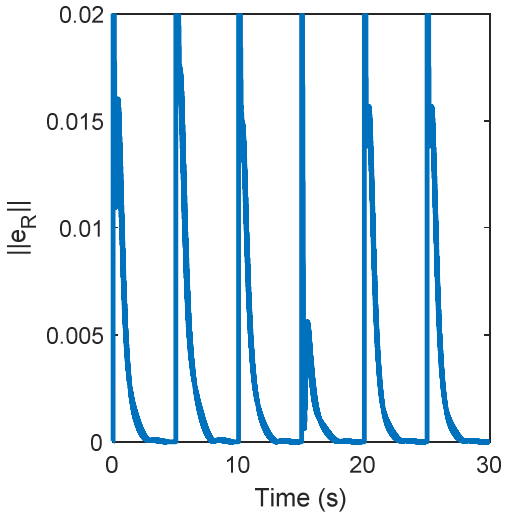

Figure 9. *Response of attitude error in attitude controller.*

With the integrator $k_i = 1.2$, the aircraft's position response is given in Figure 10. The graph showed that the steady state error returns to near zero after 7 seconds. The Euler angles and tail angle are shown in Figure 11. The rotor angular speeds are illustrated in Figure 12. The large magnitude kick is due to the large acceleration of the linearly interpolated sample trajectory. A filter can be implemented to alleviate this problem. Nevertheless, the response illustrates the fact that this nonlinear controller works with highly derivative signals, a source of which the sensor noise can enter and destabilise the problem. Until a full implementation on a physical system is completed, it is hard to estimate and/or evaluate the effects of noises, and disturbances on the system, except using several predefined mathematical models. This paves the way for further development and refinement of the method.

5. Conclusion

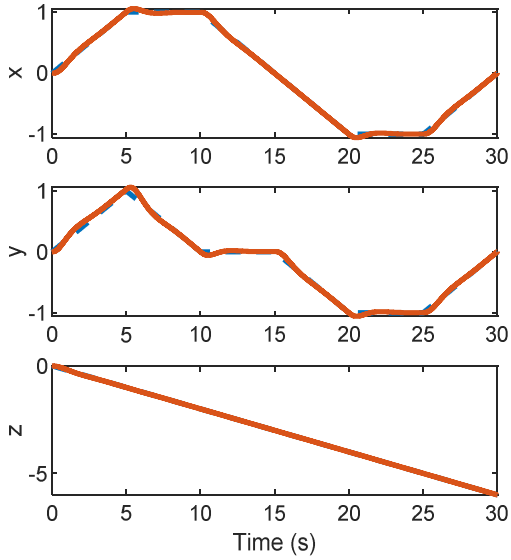

(a) Position

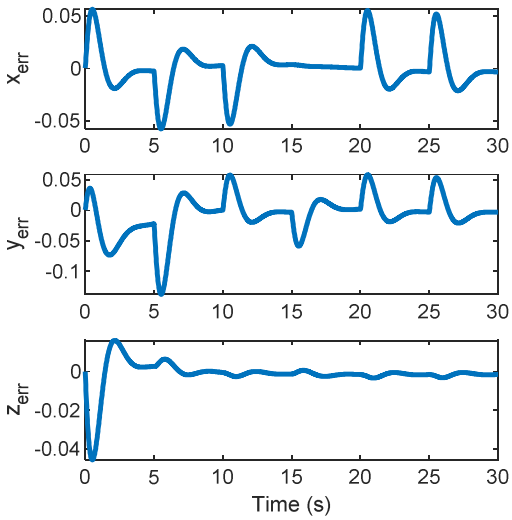

(b) Position error

Figure 10. *Aircraft's position response (with integrator) with time. Dashed lines indicate reference trajectory to track.*

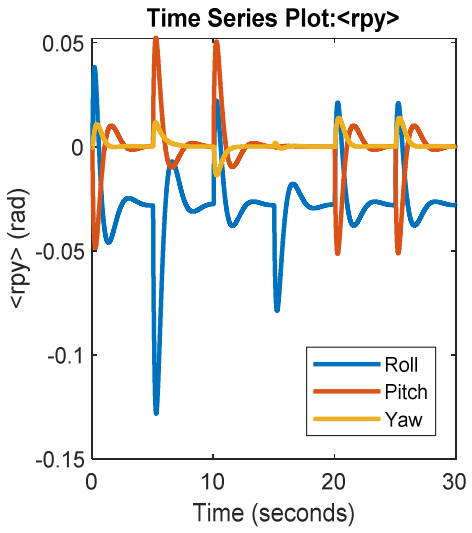

(a) Euler Angles

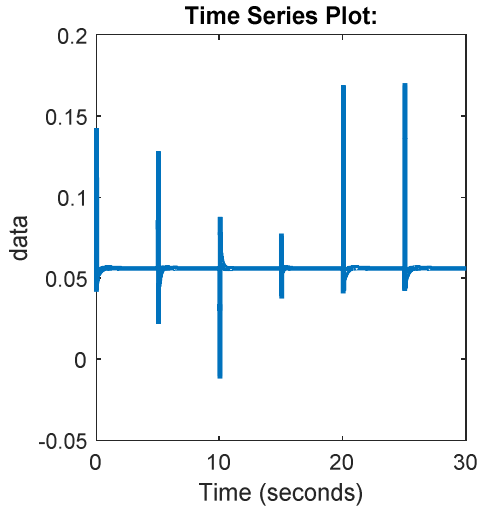

(b) Tail angle

Figure 11. *Aircraft's attitude angles and servo tail angle response.*

In this paper, we have presented a novel control algorithm adapted from the SE (3) geometric method for quadrotor UAV to control the single tri-rotor UAV. An integrator is introduced to increase the robustness, decrease the steady-state error and the stability analysis is performed by reviewing and extending the Lyapunov candidate function from [12]. The Attitude Tracking Controller exhibits almost global exponential stability, enabling agile manoeuvring capability while the Position Tracking Controller yields decent tracking performance, as illustrated in numerical simulations. However, the process of generating desired attitude is found to be quite sensitive to sensor noise, thus further attempts at implementation of different filters are required. Consideration of an integrator for attitude tracking is thought to be effective, and implementation of the entire algorithm on the microcontroller is required to study the difficulties that arise from reality. This method is also believed to be applicable for other types of autonomous vehicles, such as hexa-rotors and various kinds of Unmanned Underwater Vehicles…

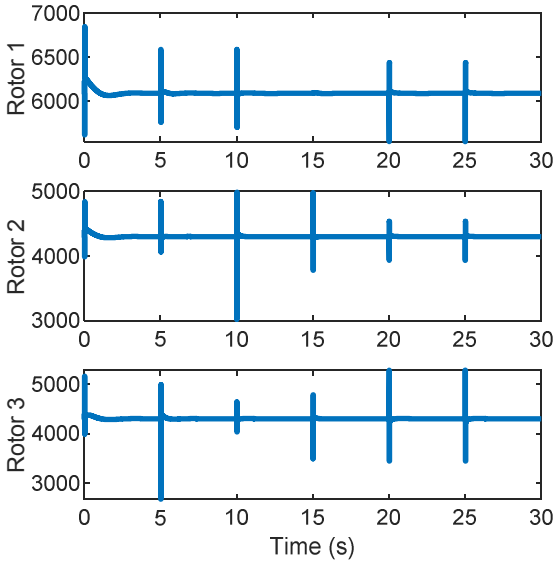

Figure 12. *Rotor angular speed during the trajectory tracking process.*

Acknowledgements

This research is funded by Vietnam National University Ho Chi Minh City (VNU-HCM) under grant number C2017-20-02.

References

[1] F. Nex and F. Remondino, "UAV for 3D mapping applications: a review," *Applied Geomatics*, vol. 6, no. 1, pp. 1–15, Aug. 2013.

[2] I. Colomina and P. Molina, "Unmanned aerial systems for photogrammetry and remote sensing: A review," *ISPRS Journal of Photogrammetry and Remote Sensing*, vol. 92, pp. 79–97, 2014.

[3] P. Liu, A. Y. Chen, Y.-N. Huang, J.-Y. Han, J.-S. Lai, S.-C. Kang, T.-H. Wu, M.-C. Wen, and M.-H. Tsai, "A review of rotorcraft Unmanned Aerial Vehicle (UAV) developments and applications in civil engineering," *Smart Structures and Systems*, vol. 13, no. 6, pp. 1065–1094, 2014.

[4] J. Escareno, A. Sanchez, O. Garcia, and R. Lozano, "Triple tilting rotor mini-UAV: Modeling and embedded control of the attitude," *2008 American Control Conference*, 2008.

[5] S. Salazar-Cruz and R. Lozano, "Stabilization and nonlinear control for a novel trirotor mini-aircraft," *Proceedings of the 2005 IEEE International Conference on Robotics and Automation*.

[6] D.-W. Yoo, H.-D. Oh, D.-Y. Won, and M.-J. Tahk, "Dynamic Modeling and Stabilization Techniques for Tri-Rotor Unmanned Aerial Vehicles," *International Journal of Aeronautical and Space Sciences*, vol. 11, no. 3, pp. 167–174, 2010.

[7] J.-S. Chiou, H.-K. Tran, and S.-T. Peng, "Attitude Control of a Single Tilt Tri-Rotor UAV System: Dynamic Modeling and Each Channels Nonlinear Controllers Design," *Mathematical Problems in Engineering*, vol. 2013, pp. 1–6, 2013.

[8] Z. Ali, D. Wang, and M. Aamir, "Fuzzy-Based Hybrid Control Algorithm for the Stabilization of a Tri-Rotor UAV," *Sensors*, vol. 16, no. 5, p. 652, Sep. 2016.

[9] F. K. Yeh, C. W. Huang, J. J. Huang, "Adaptive fuzzy sliding-mode control for a mini-UAV with propellers", *SICE Annual Conference (SICE), 2011 Proceedings of,* pp. 645-650, 2011.

[10] A. Kulhare, A. B. Chowdhury, and G. Raina, "A back-stepping control strategy for the Tri-rotor UAV," *2012 24th Chinese Control and Decision Conference (CCDC)*, 2012.

[11] M. K. Mohamed and A. Lanzon, "Design and control of novel tri-rotor UAV," *Proceedings of 2012 UKACC International Conference on Control*, 2012.

[12] T. Lee, M. Leok, and N. H. Mcclamroch, "Geometric tracking control of a quadrotor UAV on SE (3)," *49th IEEE Conference on Decision and Control (CDC)*, 2010.

[13] T. Fernando, J. Chandiramani, T. Lee, and H. Gutierrez, "Robust adaptive geometric tracking controls on SO (3) with an application to the attitude dynamics of a quadrotor UAV," *IEEE Conference on Decision and Control and European Control Conference*, 2011.

[14] T. D. Hoang, "Application and simulation of nonlinear geometric control for Quadrotor UAVs," *Graduation Thesis – Ho Chi Minh City University of Technology,* 2018.

[15] T. D. Hoang, "An experiment with integration in deriving Lyapunov candidate based on integral back-stepping technique," unpublished.